

Nucleon form factors with 2+1 flavors of DWF and All-Mode-Averaging

Meifeng Lin

With: Yasumichi Aoki, Tom Blum, Taku Izubuchi, Chulwoo Jung, Shigemi Ohta, ,
Shoichi Sasaki, Eigo Shintani, Takeshi Yamazaki

The 31 International Symposium on Lattice Field Theory
Mainz, Germany, July 29 – August 3, 2013

Outline

- Introduction
- Numerical Details
- Error Reduction with All-Mode-Averaging
- Results



Introduction

- Nucleon Dirac and Pauli form factors, $F_1^N(Q^2)$ and $F_2^N(Q^2)$ respectively, are defined through the nucleon vector matrix elements,

$$\langle N(p') | J_\mu^N(x) | N(p) \rangle = e^{i(p'-p) \cdot x} \bar{u}(p') \left[\gamma_\mu F_1^N(Q^2) + i \sigma_{\mu\nu} \frac{q_\nu}{2M_N} F_2^N(Q^2) \right] u(p)$$

- p and p' are the initial and final momenta of the nucleon, respectively. $Q^2 = -(p'-p)^2$ is the momentum transfer from the incoming nucleon to the outgoing nucleon.
- The Dirac and Pauli form factors are related to the electric and magnetic Sachs form factors by

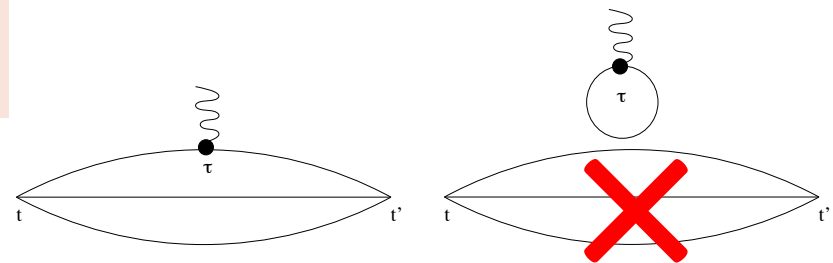
$$G_E(Q^2) = F_1(Q^2) - \frac{Q^2}{4M_N^2} F_2(Q^2)$$

$$G_M(Q^2) = F_1(Q^2) + F_2(Q^2)$$

- Two types of contractions contribute.

Consider only the connected contributions.

→ Isovector (p-n) observables have only connected contributions.



Why are we interested?

- They encode the charge, magnetic moment and size (mean square radii) of the nucleon:

$$e_N = F_1^N(0)$$
$$\kappa_N = F_2^N(0) = \mu_N - 1$$
$$\langle r_i^2 \rangle = -6 \frac{dF_i(Q^2)}{dQ^2} \Big|_{Q^2=0}$$

- The Proton Size Puzzle** from the experiment: The proton size measured from muonic hydrogen Lamb shift is **7 sigma's** smaller than the CODATA *e-p scattering* result.

PDG2013

<u>VALUE (fm)</u>	<u>DOCUMENT ID</u>	<u>TECN</u>	<u>COMMENT</u>
0.84087 ± 0.00026 ± 0.00029	ANTOIGNINI	13	LASR μp -atom Lamb shift
0.8775 ± 0.0051	MOHR	12	RVUE 2010 CODATA, <i>e p</i> data

- Ab initio* lattice calculations can provide QCD contributions.

Systematic errors that need to be addressed

- Chiral extrapolation errors:
 - Most of the lattice calculations to date are done at pion masses heavier than the physical value. If the pion masses are too heavy, chiral extrapolations may not be reliable.
 - More and more lattice calculations recently have pushed the pion masses to be closer to or even directly at 140 MeV, so this source may not be as big an issue as before.
- Finite volume effects:
 - If the lattice is too small, we may need to worry about finite volume effects.
 - At least two volumes are needed to address this issue directly. Or simulate at a very large box, but we don't know how large is sufficient *a priori*.
- Excited-state contaminations:
 - Nucleon ground state dominates only at large-enough Euclidean time. If the separation is not sufficient, we may see effects of the excited states.
 - Need at least two source-sink separations to estimate the contaminations.
- Other effects: discretization errors, isospin symmetry breaking, etc.

Our calculations

- We attempt to minimize at least the first three sources of systematic errors by
 - Going to pion masses as light as 170 MeV.
 - Using a large physical volume of $(4.6\text{fm})^3$.
 - Applying two source-sink separations.
- Gauge ensembles [generated by RBC and UKQCD Collaborations]:
 - Gauge action: Iwasaki + Dislocation-Suppressing-Determinant-Ratio, $\beta=1.75$.
 - Fermion action: Standard domain wall fermions, $L_s = 32 \rightarrow m_{\text{res}} \approx 0.0018$.
 - 1 lattice volume: $32^2 \times 64$.
 - 1 lattice spacing: $a^{-1} = 1.37(1) \text{ GeV} \rightarrow a \approx 0.144 \text{ fm}$.
 - 2 pion masses: $M_\pi \approx 170 \text{ MeV}$ and 250 MeV .
- Nucleon three-point function details:
 - Source: Gaussian smearing, width = 6 lattice units for 70 steps + APE link smearing.
 - Source-sink separations:
 - $t_{\text{snk}} - t_{\text{src}} = 1.0 \text{ fm}$ and 1.3 fm for $M_\pi \approx 170 \text{ MeV}$,
 - $t_{\text{snk}} - t_{\text{src}} = 1.3 \text{ fm}$ only for 250 MeV .

RBC and UKQCD Collaborations

RBC		UKQCD	
Ziyuan Bai	Meifeng Lin	Rudy Arthur	Richard Kenway
Thomas Blum	Robert Mawhinney	Peter Boyle	Andrew Lytle
Norman Christ	Greg McGlynn	Hei-Man Choi	Marina Marinkovic
Tomomi Ishikawa	David Murphy	Luigi Del Debbio	Enrico Rinaldi
Taku Izubuchi	Shigemi Ohta	Shane Drury	Brian Pendleton
Luchang Jin	Eigo Shintani	Jonathan Flynn	Antonin Portelli
Chulwoo Jung	Amarjit Soni	Julien Frison	Chris Sachrajda
Taichi Kawanai	Oliver Witzel	Nicolas Garron	Ben Samways
Chris Kelly	Hantao Yin	Jamie Hudspith	Karthee Sivalingam
Hyung-Jin Kim	Jianglei Yu	Tadeusz Janowski	Matthew Spraggs
Christoph Lehner	Daiqian Zhang	Andreas Juettner	Tobi Tsang
Jasper Lin			



Nucleon Three-point Functions

- ▶ We use the standard proton interpolating operator, with smearing $S = \text{Gaussian (G) or Local (L)}$

$$\chi_S(x) = \epsilon_{abc} \left([u_a^S(x)]^T C \gamma_5 d_b^S(x) \right) u_c^S(x)$$

- ▶ Nucleon two-point functions:

$$C_S(t - t_{src}, p) = \sum_{\vec{x}} e^{i\vec{p} \cdot \vec{x}} \text{Tr} \left[\mathcal{P}_4 \langle 0 | \chi_S(\vec{x}, t) \bar{\chi}_G(\vec{0}, t_{src}) | 0 \rangle \right]$$

- ▶ Nucleon three-point functions:

$$C_{J_\mu}^{\mathcal{P}_\alpha} = \sum_{\vec{x}, \vec{z}} e^{i\vec{q} \cdot \vec{z}} \text{Tr} \left[\mathcal{P}_\alpha \langle 0 | \chi_G(\vec{x}, t_{snk}) J_\mu(\vec{z}, t) \bar{\chi}_G(\vec{0}, t_{src}) | 0 \rangle \right]$$

with the projection operators:

$$\begin{aligned} \mathcal{P}_4 &= (1 + \gamma_4)/2 \\ \mathcal{P}_{53} &= (1 + \gamma_4)\gamma_5\gamma_3/2 \end{aligned}$$

Determining the form factors

- The form factors are determined from the ratio:

$$R_{J_\mu}^{\mathcal{P}\alpha}(q, t) = K \cdot \frac{C_{J_\mu}^{\mathcal{P}\alpha}(\vec{q}, t)}{C_G(t_{\text{snk}} - t_{\text{src}}, 0)} \left[\frac{C_L(t_{\text{snk}} - t, q) C_G(t - t_{\text{src}}, 0) C_L(t_{\text{snk}} - t_{\text{src}}, 0)}{C_L(t_{\text{snk}} - t, 0) C_G(t - t_{\text{src}}, q) C_L(t_{\text{snk}} - t_{\text{src}}, q)} \right]^{1/2},$$

with

$$K = M_N \sqrt{2E(q)(M_N + E(q))}$$

- ▶ The ratios conveniently defined to be directly related to the Sachs Form Factors:

$$G_E(q, t) = \frac{R_{V_4}^{\mathcal{P}4}(q, t)}{M_N(M_N + E(q))},$$

$$G_M(q, t) = \frac{1}{2} \left(\frac{R_{V_1}^{\mathcal{P}53}(q, t)}{q_2 M_N} - \frac{R_{V_2}^{\mathcal{P}53}(q, t)}{q_1 M_N} \right),$$

- ▶ And the Dirac and Pauli form factors can be obtained by:

$$F_1(q^2) = \frac{G_E(q) + \tau G_M(q)}{1 + \tau}, \text{ for all } q$$

$$F_2(q^2) = \frac{G_M(q) - G_E(q)}{1 + \tau}, \text{ for } q \neq 0$$

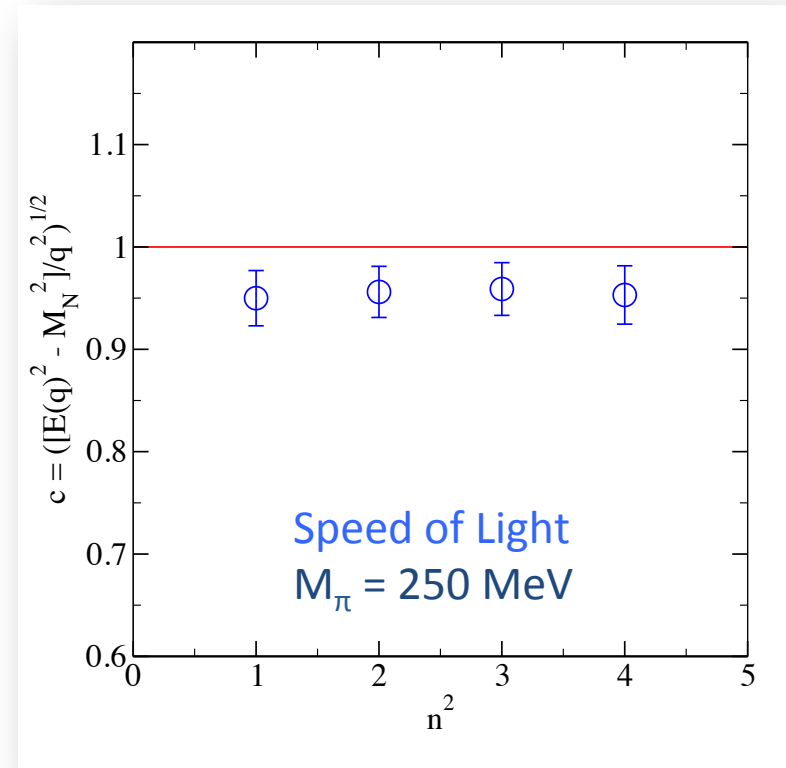
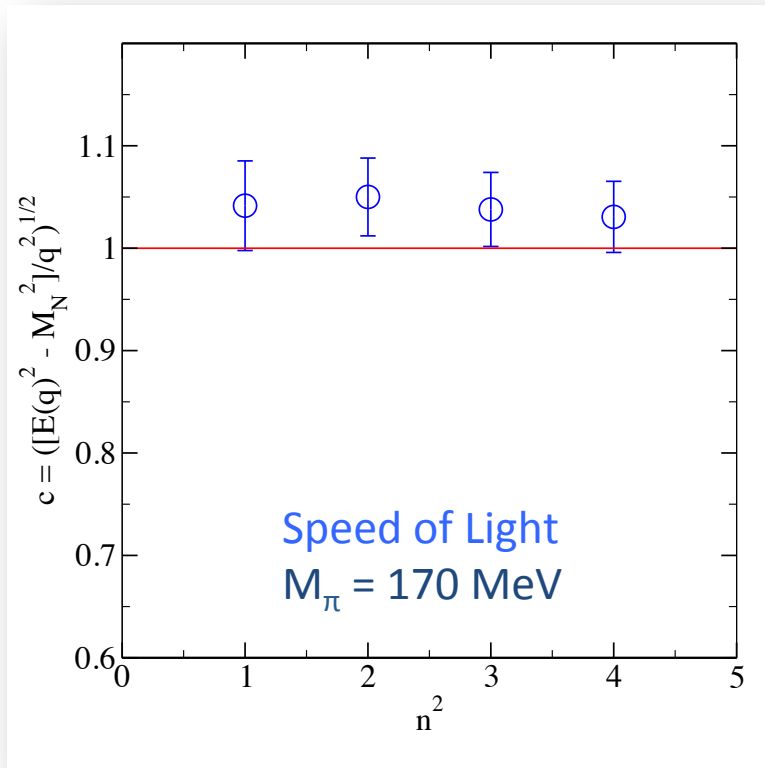
where $\tau = q^2/(4M_N^2)$.

Nucleon Dispersion relation

- One question is: **what should we use for $E(q)$?**
 - It can be directly determined from the nucleon two-point function.
 - Or we can use the nucleon dispersion relation

Difference is small.

$$E(q) = \sqrt{M_N^2 + \vec{q}^2} = \sqrt{M_N^2 + \vec{n}^2 (2\pi)^2 / L^2}$$



Error Reduction with All-Mode-Averaging

- Nucleon signal-to-noise decreases exponentially with decreasing pion mass due to 3-pion contributions.

$$\frac{\text{signal}}{\text{noise}} \propto \sqrt{N} e^{-(M_N - \frac{3}{2}M_\pi)t}$$

- To reduce the statistical errors on the light, $M_\pi = 170$ MeV, ensemble, we employed the All-Mode-Averaging technique [Blum, Izubuchi, Shintani, arXiv: 1208.4349]

$$\begin{aligned} \mathcal{O}^{(\text{imp})} &= \mathcal{O}^{(\text{rest})} + \mathcal{O}_G^{(\text{appx})}, \\ \mathcal{O}^{(\text{rest})} &= \mathcal{O} - \mathcal{O}^{(\text{appx})}, \quad \mathcal{O}_G^{(\text{appx})} = \frac{1}{N_G} \sum_{g \in G} \mathcal{O}^{(\text{appx}),g} \end{aligned}$$

- Takes advantage of the covariant transformation G of the lattice to use many sources.
- Needs to construct an approximate operator $\mathcal{O}^{(\text{appx})}$ which has strong correlation with the exact operator \mathcal{O} .
- $\mathcal{O}^{(\text{appx})}$ needs to be much cheaper to calculate than \mathcal{O} .

All Mode Averaging

- In our application, we take advantage of the translational invariance of the lattice, and use sources on
 - 7 time slices and 16 spatial source shifts on each time slice = 112 measurements/config
- The approximation operator is constructed from low-mode deflated sloppy quark propagator:

$$S_{approx} = S_l^{\parallel} + S_{sloppy}^{\perp}$$

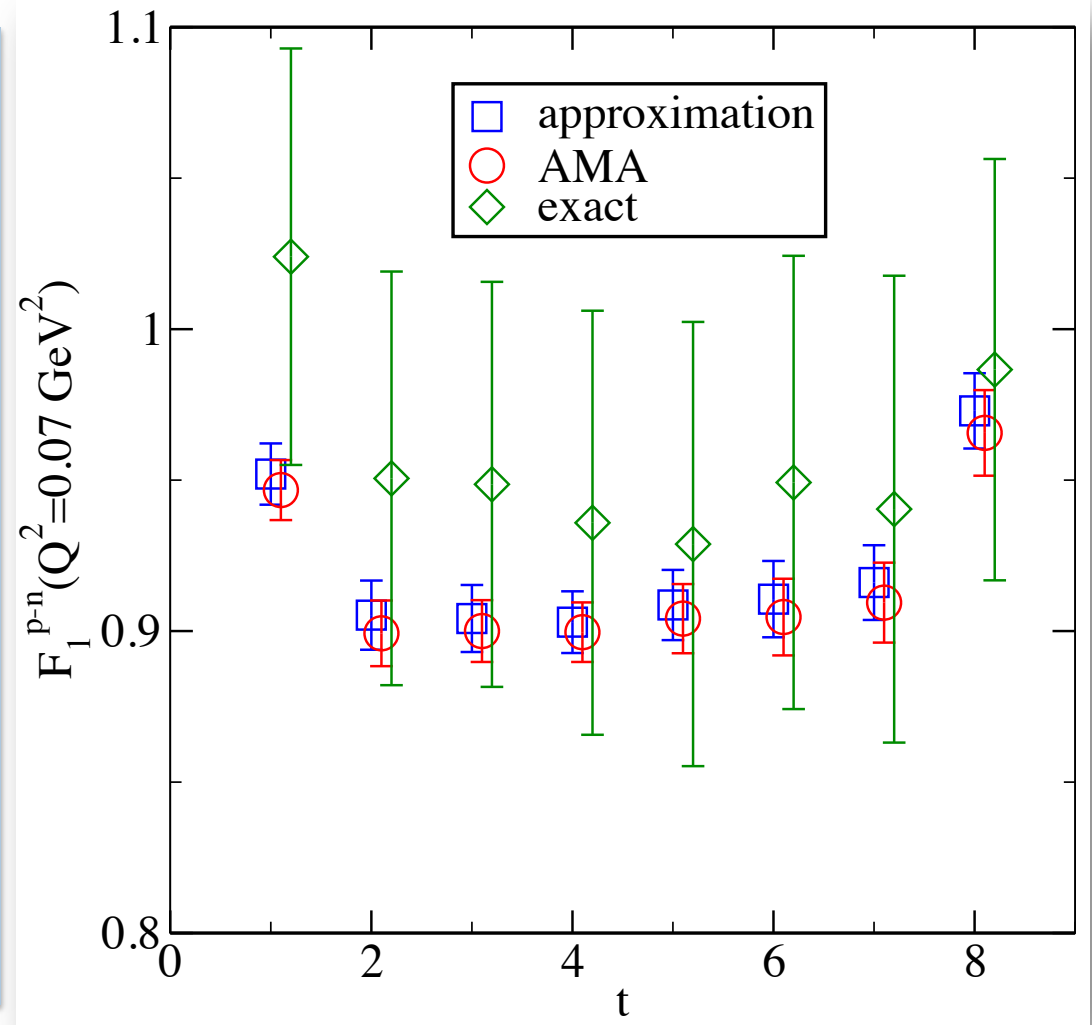
- 1000 low eigenmodes are calculated to construct the low-mode part of the propagator . The low-mode deflated propagator is determined from sloppy CG with a stopping condition of $O(10^{-3})$.
- Correct for the bias by the exact, but calculated less frequently, operator:

$$O_{AMA} = \frac{1}{N_{approx}} \sum_{i=1}^{N_{approx}} O_{approx}^i + \frac{1}{N_{exact}} \sum_{j=1}^{N_{exact}} (O_{exact}^j - O_{approx}^j), N_{exact} \ll N_{approx}$$

- To reduce the cost even further, Möbius DWF is used with smaller $L_s = 16$ for S_{approx} .

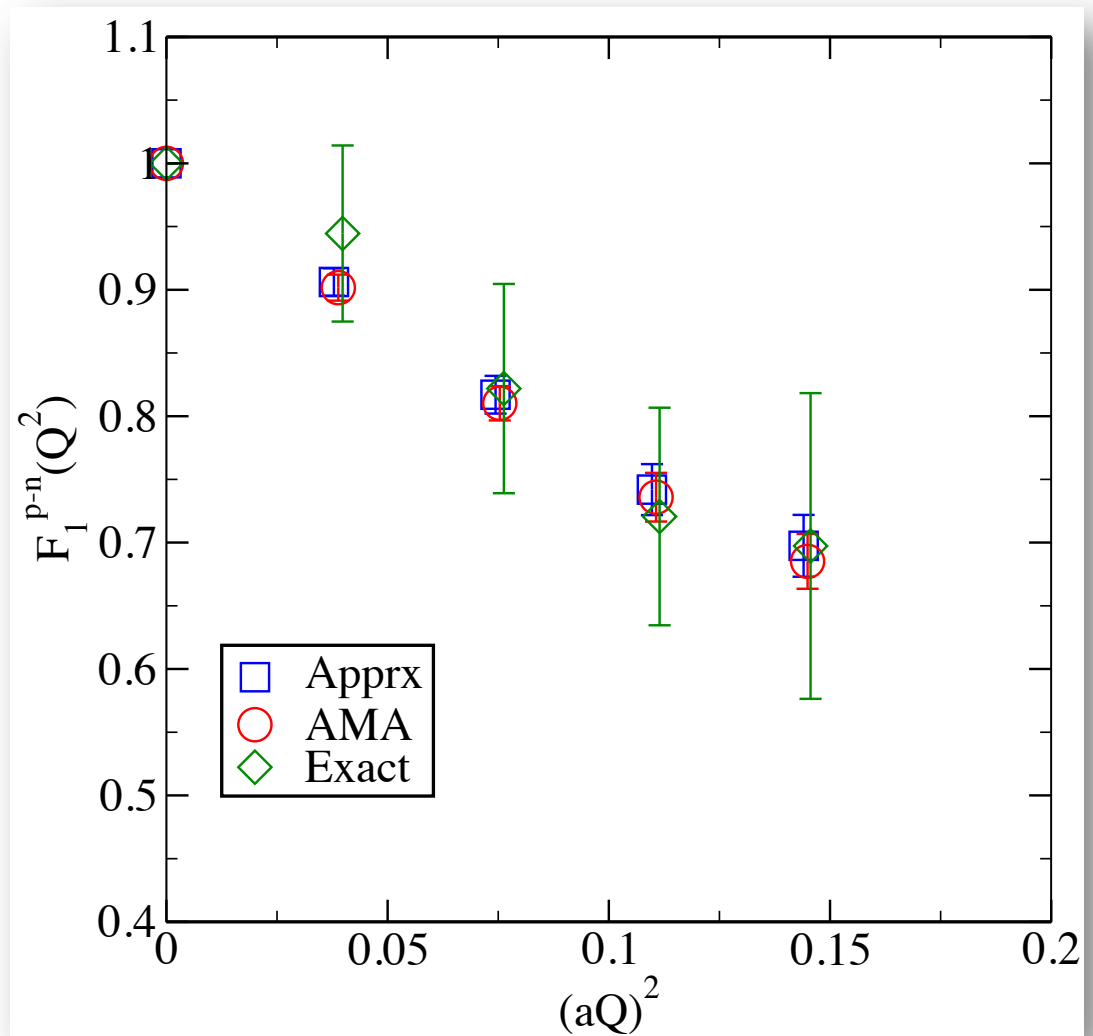
Example

- 170 MeV, 39 configurations
- 112 sources per configuration for the approximation.
- 4 sources per configuration for the exact solution.
- **One approximate propagator is 1/65 of the cost of the exact propagator.** (taking into account the cost for the low modes)

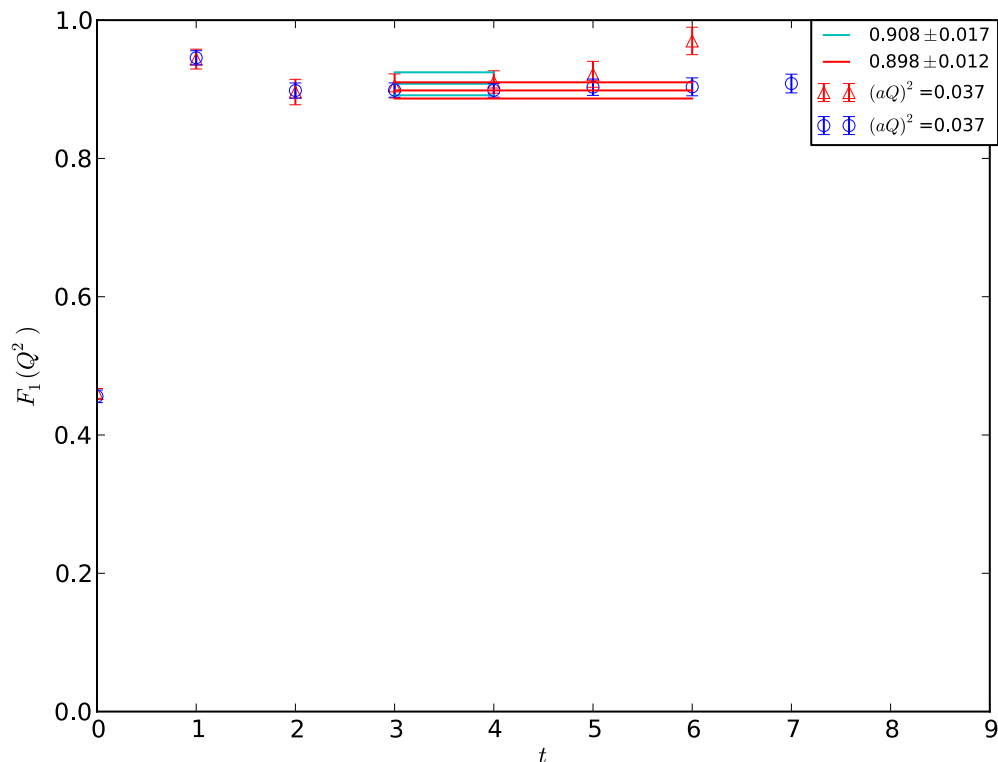


Speedup Estimate

- Error reduction is 4.6x – 6.4x over the Q^2 range.
- Would need 21x to 41x more statistics to achieve the same error reduction with the exact calculation.
- Actual AMA cost = 1.4x
- Speedup is 15x to 29x!

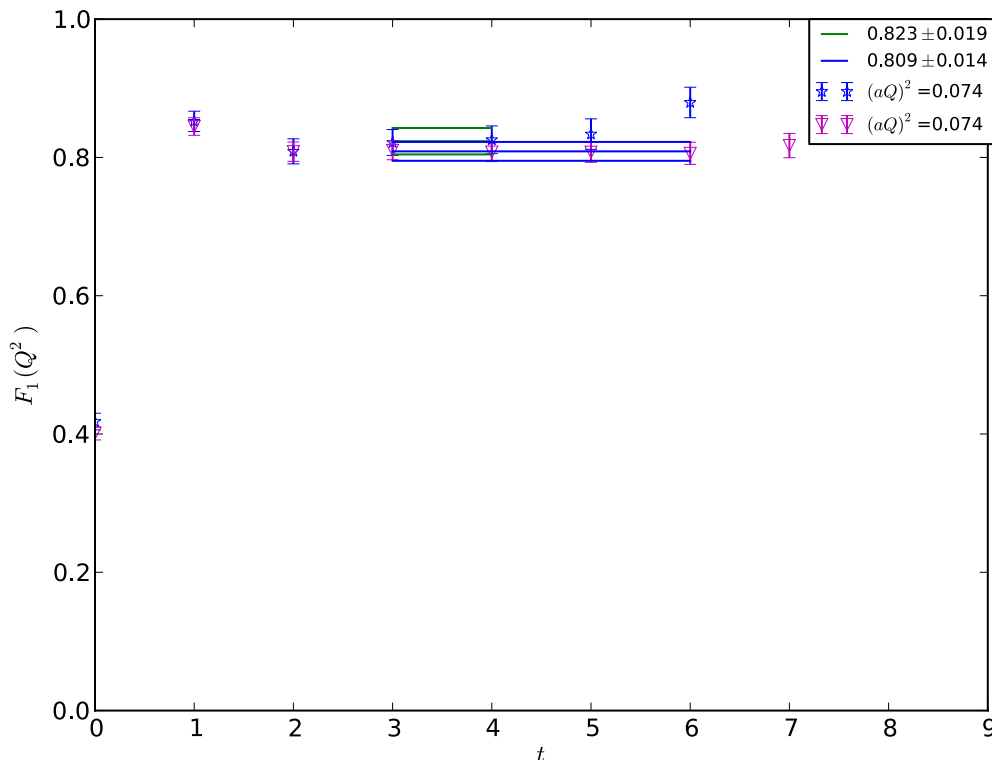


(Lack of) Excited-state Contaminations?



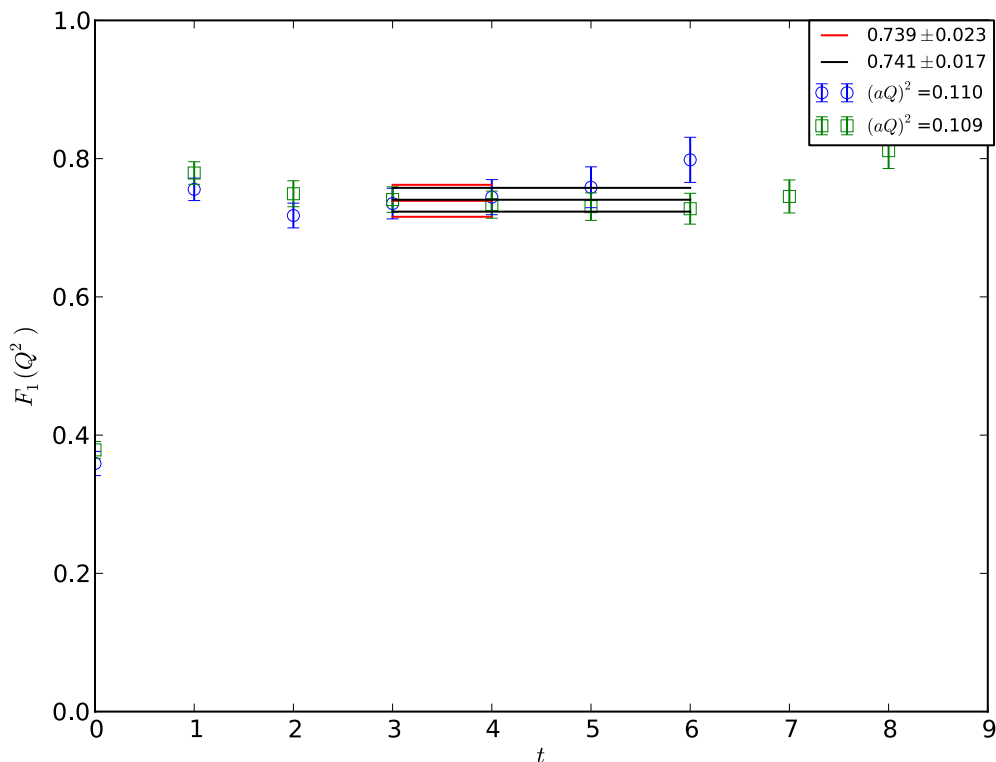
- AMA also allows us to calculate with different source-sink separations with little additional cost, since we can use the same low eigenmodes.
- **Shorter separation of 1fm:**
 - 8 configurations
 - 64 sources with sloppy CG
 - 1 source with exact solution
- **No visible difference. Excited-state contaminations are small.**

(Lack of) Excited-state Contaminations?



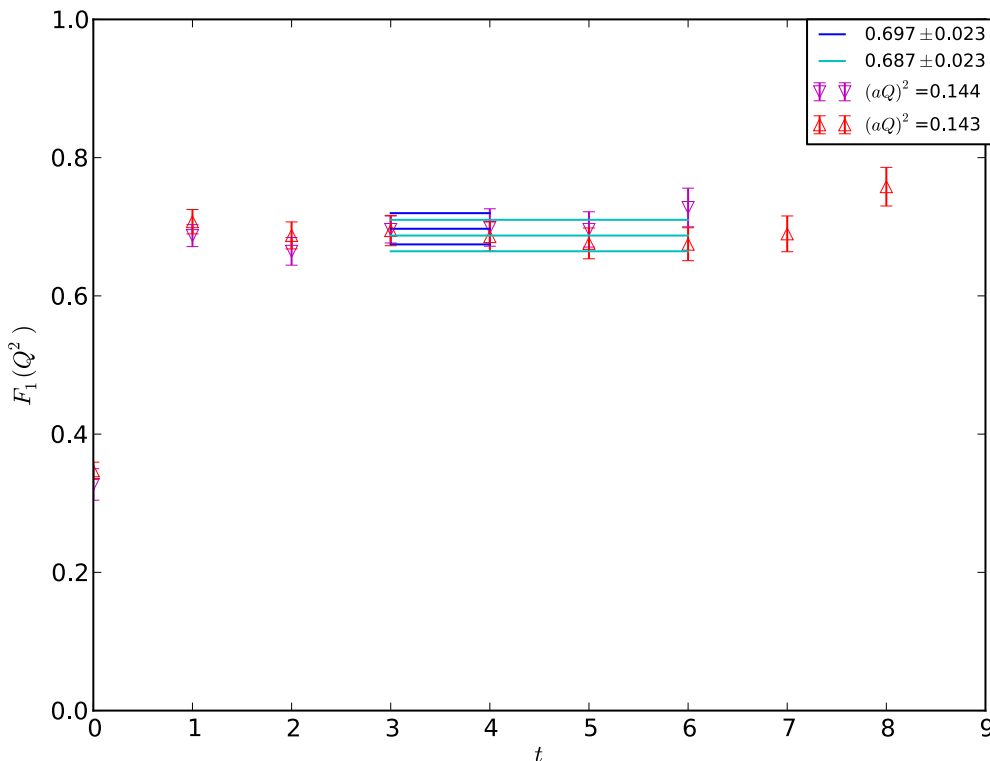
- AMA also allows us to calculate with different source-sink separations with little additional cost, since we can use the same low eigenmodes.
- **Shorter separation of 1fm:**
 - 8 configurations
 - 64 sources with sloppy CG
 - 1 source with exact solution
- **No visible difference. Excited-state contaminations are small.**

(Lack of) Excited-state Contaminations?



- AMA also allows us to calculate with different source-sink separations with little additional cost, since we can use the same low eigenmodes.
- **Shorter separation of 1fm:**
 - 8 configurations
 - 64 sources with sloppy CG
 - 1 source with exact solution
- **No visible difference. Excited-state contaminations are small.**

(Lack of) Excited-state Contaminations?



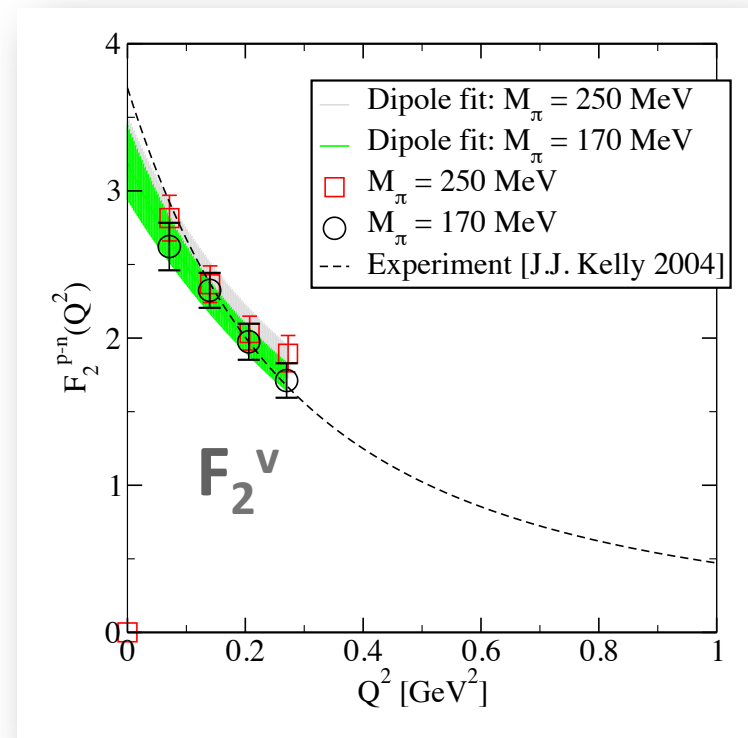
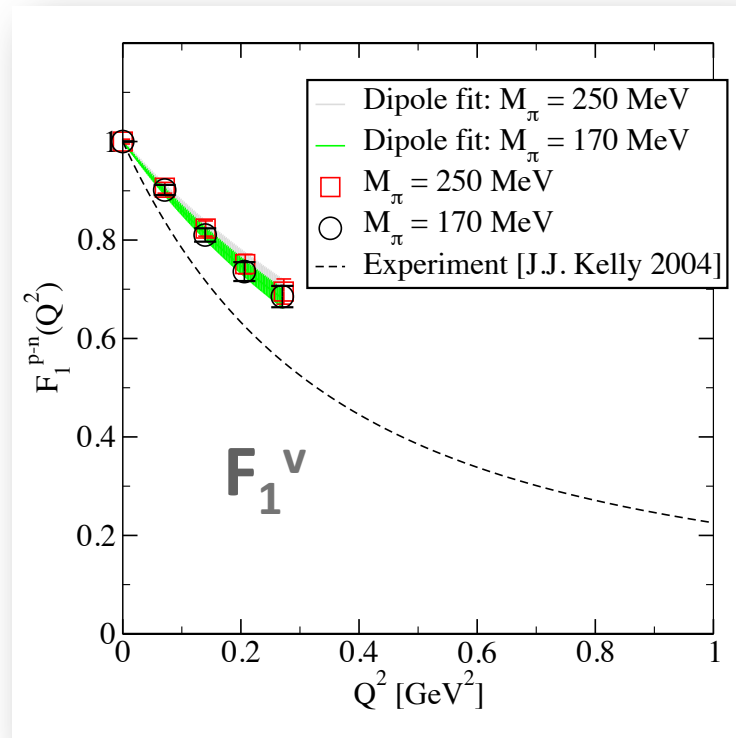
- AMA also allows us to calculate with different source-sink separations with little additional cost, since we can use the same low eigenmodes.
- **Shorter separation of 1fm:**
 - 8 configurations
 - 64 sources with sloppy CG
 - 1 source with exact solution
- **No visible difference. Excited-state contaminations are small.**

Q^2 dependence

- The empirical dipole form describes the Q^2 dependence of the data very well:

$$F_i(Q^2) = \frac{F_i(0)}{(1 + Q^2 / M_i^2)^2}$$

- RMS radii are determined as: $\langle r_i^2 \rangle = 12 / M_i^2$

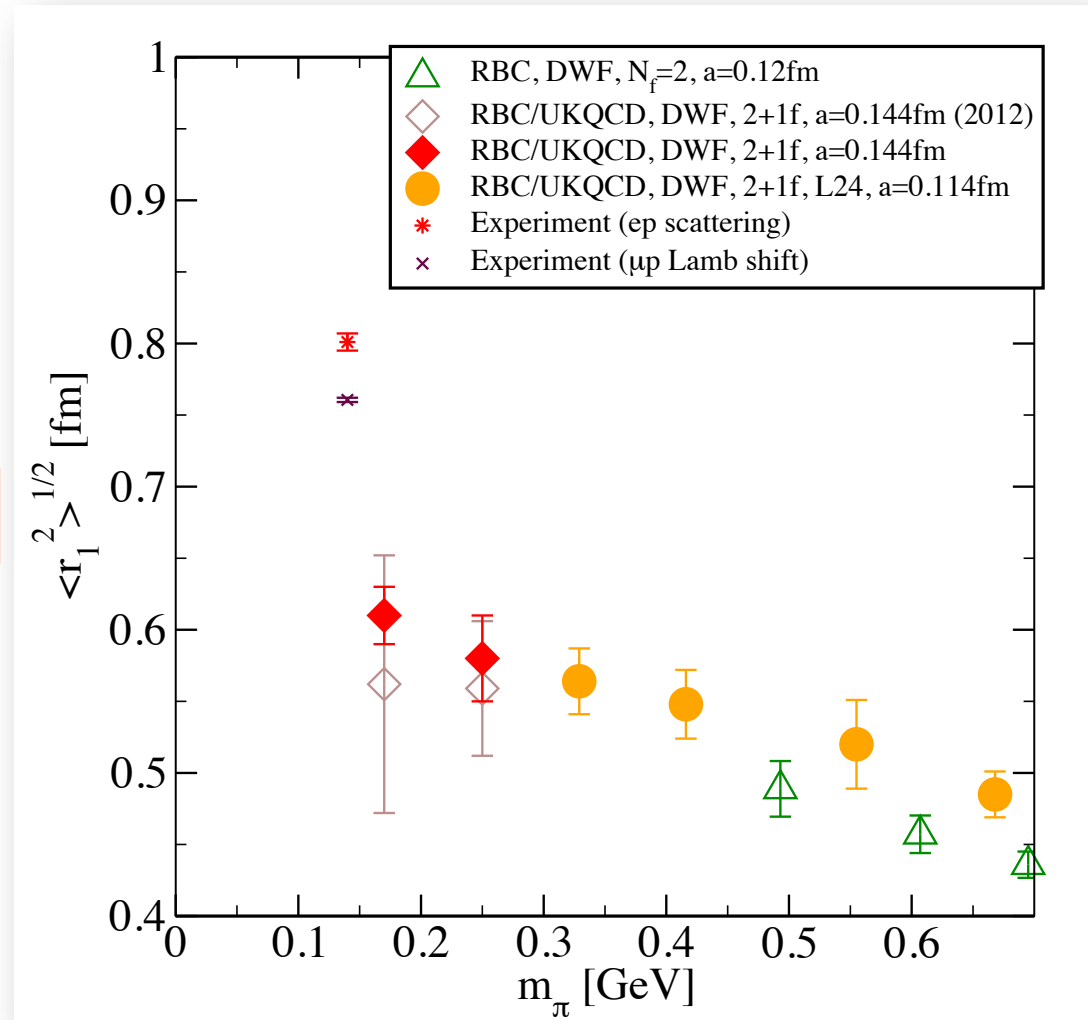


Results

- The isovector Dirac radius is related to the proton and neutron electric charge radii .

$$\langle (r_1^v)^2 \rangle = \langle (r_E^p)^2 \rangle - \langle (r_E^n)^2 \rangle - \left(\frac{6}{4M_p^2} \kappa^p - \frac{6}{4M_n^2} \kappa^n \right)$$

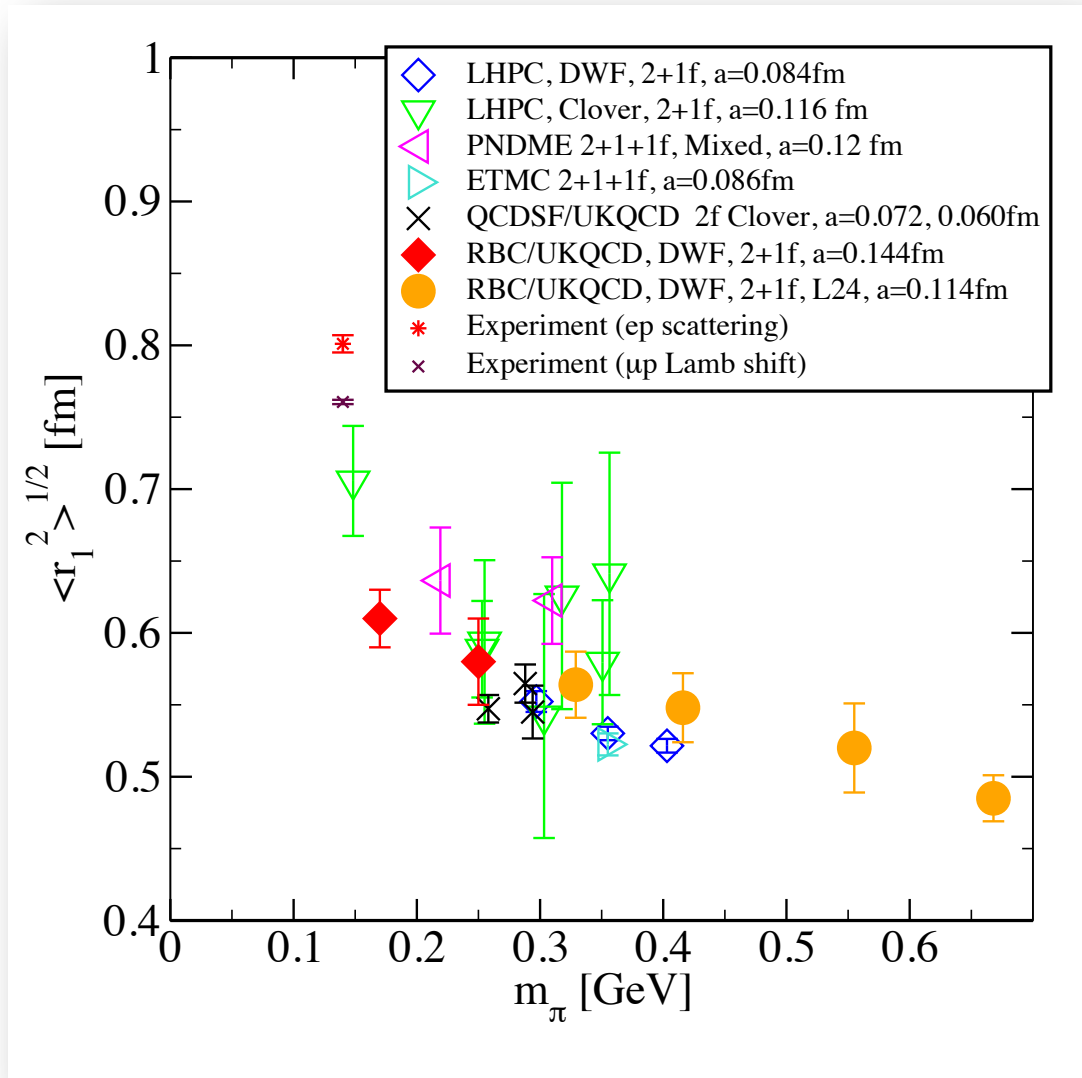
- AMA reduced the statistical errors substantially on the lighter mass point.



RBC/UKQCD DWF Results

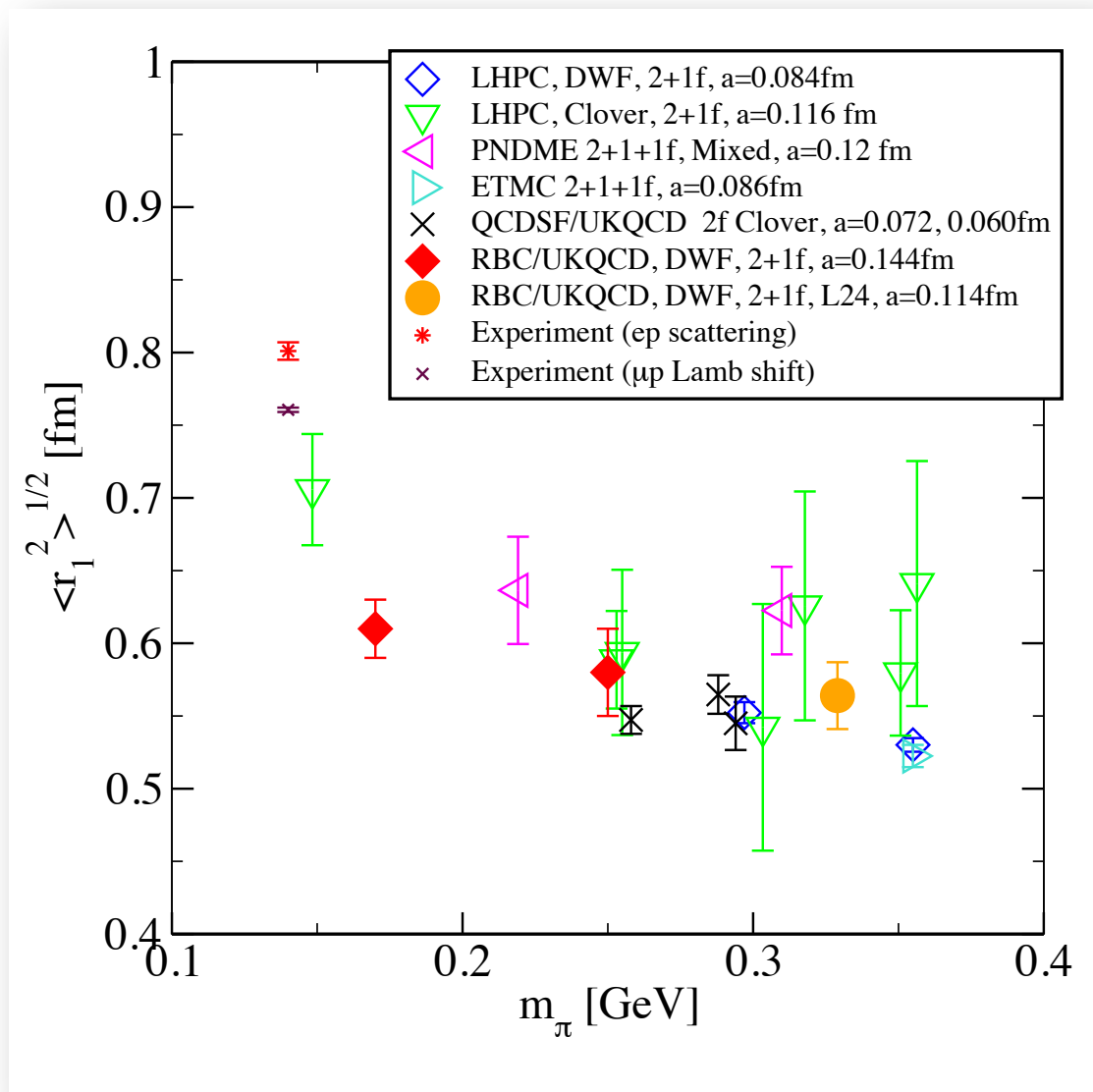
Other Lattice Results

- The recent lattice results are in reasonable agreement.
- Global data show an upward trend towards the physical limit.



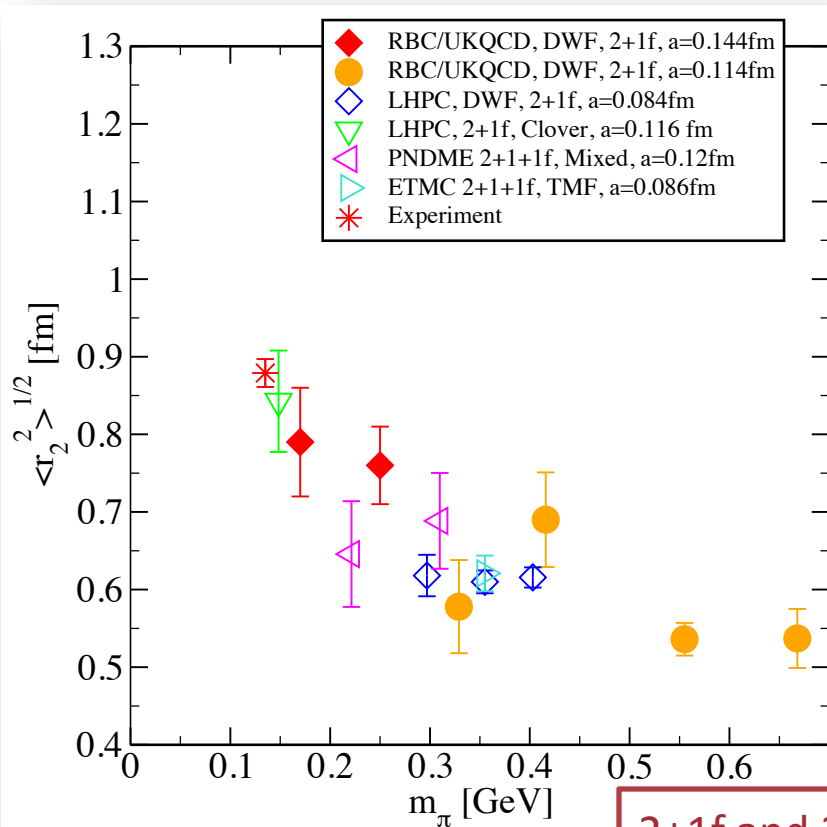
Partial compilation of global results

A closer look at the light mass region

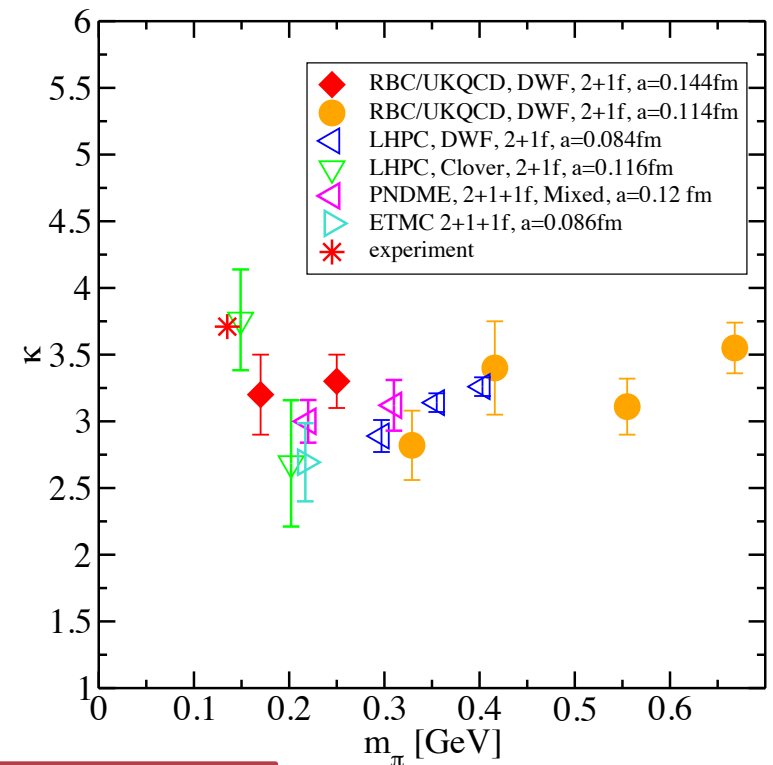


Derived quantities from F_2

Isvector Pauli Radii



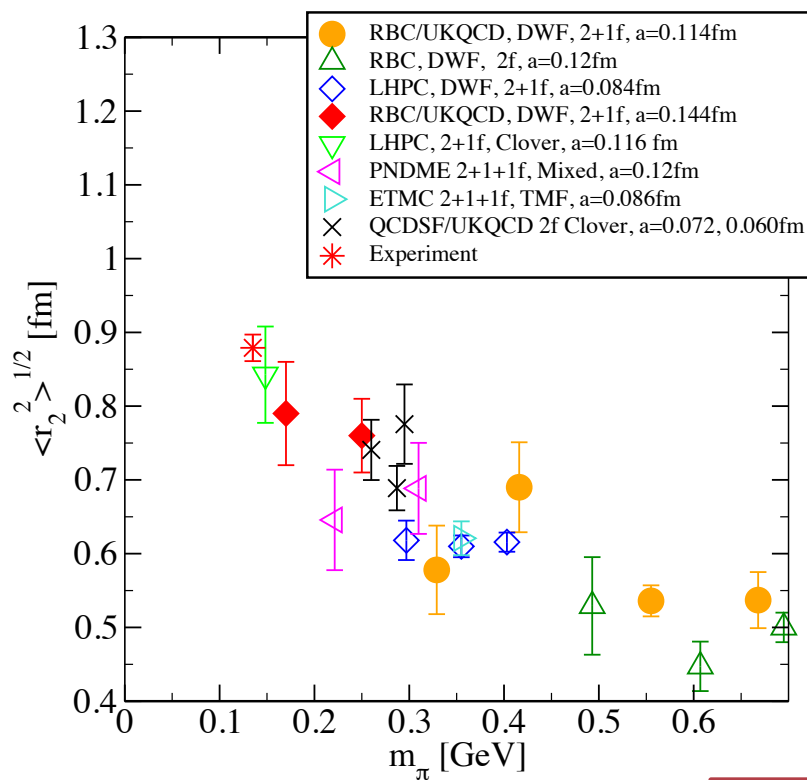
Anomalous Magnetic Moment



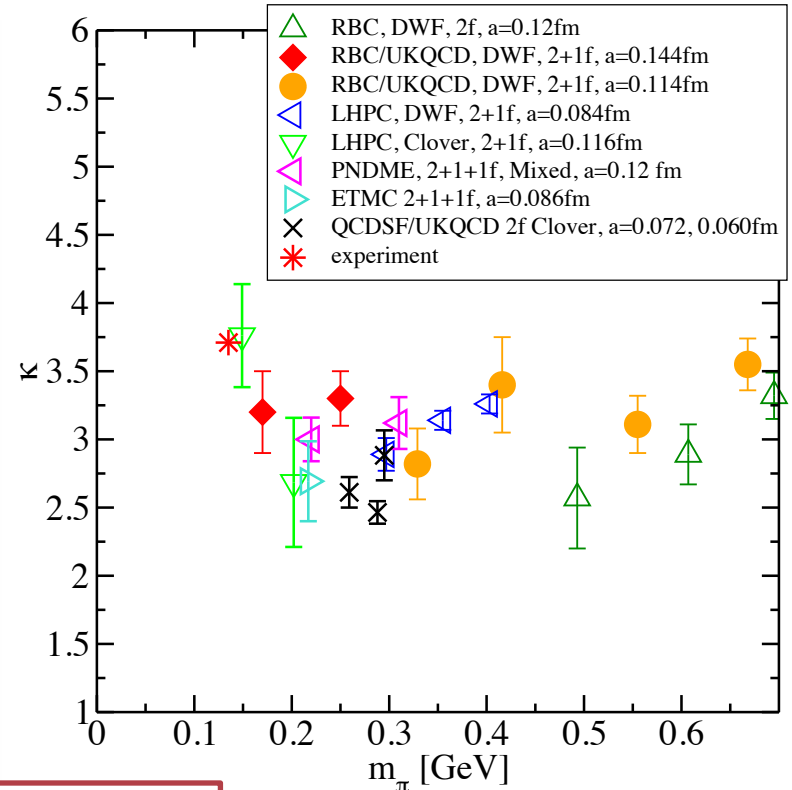
2+1f and 2+1+1f results only

Including 2f Results

Isovector Pauli Radii



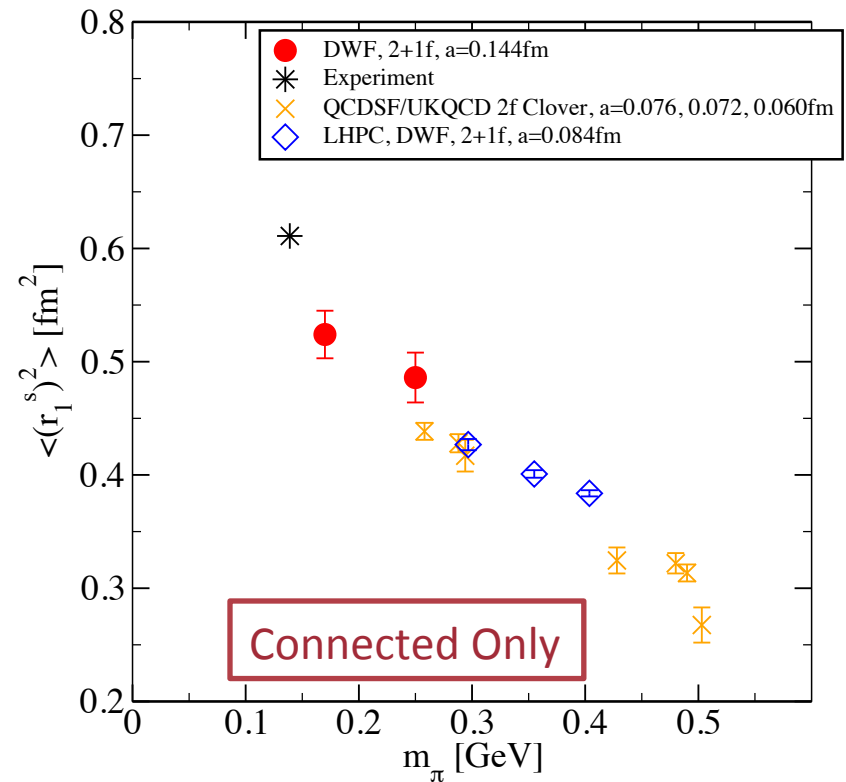
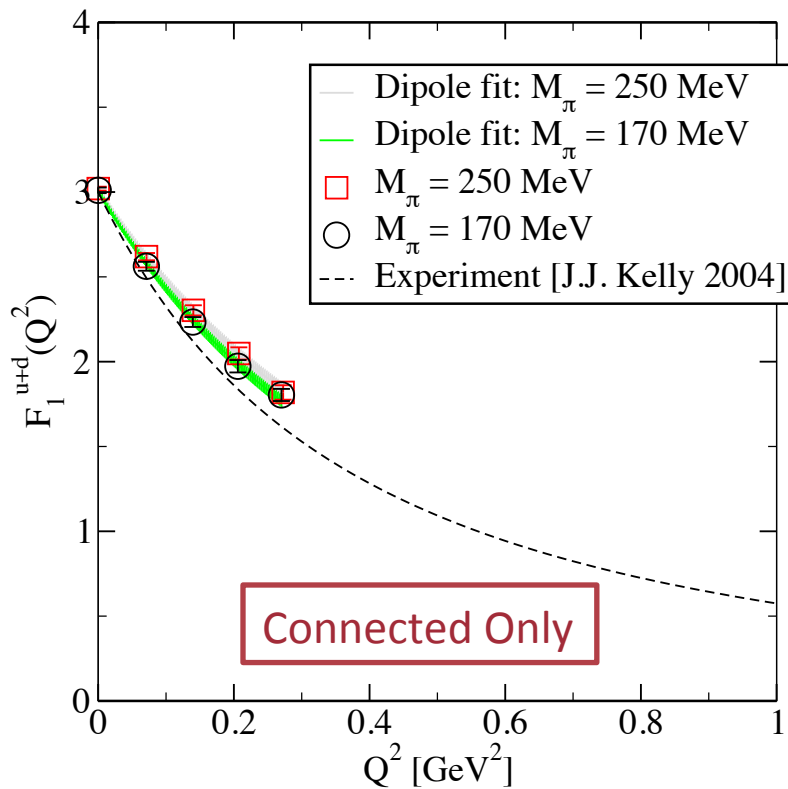
Anomalous Magnetic Moment



Including 2f results

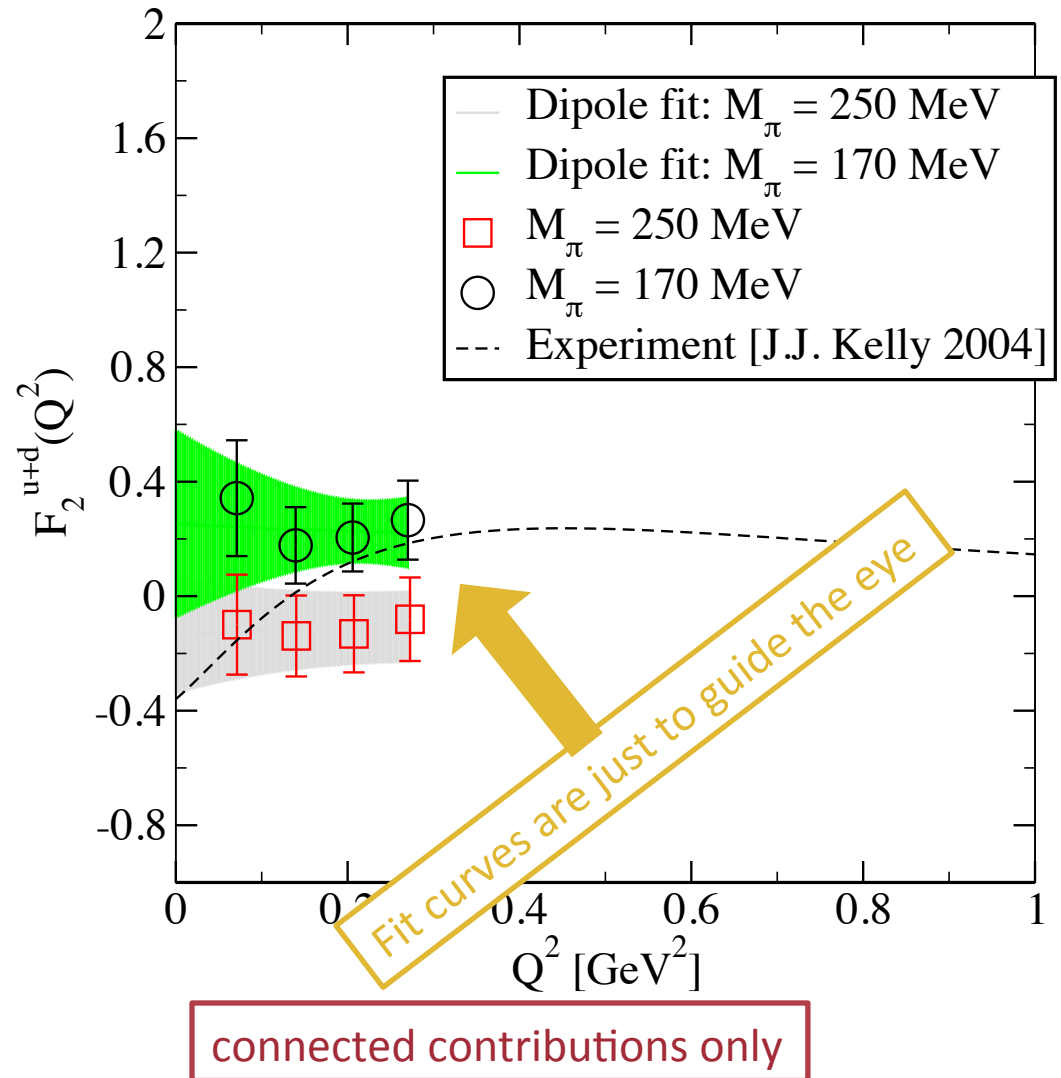
Isoscalar Dirac Form Factors and Radii (connected contributions only)

- Connected contributions to the isoscalar Dirac form factors are getting close to the experiment.



Isoscalar Pauli Form Factors

- $F_2^s(Q^2)$ has little Q^2 dependence.
- Data are still noisy.
- Magnitude is consistent with the experiment.
- Extracting the radii and the anomalous magnetic moment not possible at the moment.



What's Next?

- Chiral extrapolations.
- Estimating systematic errors: finite volume, discretization, etc.
- Disconnected diagrams.

- RBC and LHPC are joining forces to calculate nucleon structure observables directly at the physical pion mass.
 - New physical-pion-mass 2+1 flavor Domain Wall ensembles are being generated jointly by the RBC and UKQCD Collaborations. [see Bob Mawhinney's talk on Thursday]
 - $a=0.086$ fm, $64^3 \times 128$
 - $a=0.114$ fm, $48^3 \times 96$

Conclusions

- AMA is very effective in reducing statistical errors, with computational speedup of a factor of 15 to 29 in our applications.
- We are now able to achieve 3-4% statistical errors on many quantities such as g_A and charge radius at 170 MeV pion with domain wall fermions.
- The lighter pion mass results show a very encouraging trend to approach the experimental values, but chiral extrapolations are still needed to do a quantitative comparison.
- Calculations directly at the physical pion mass are coming up.

Acknowledgments

- The gauge configurations used were generated by the RBC and UKQCD Collaborations using BlueGene/P supercomputers at Argonne Leadership Computing Facility, Brookhaven National Laboratory, University of Edinburgh and RIKEN-BNL Research Center.
- The majority of the correlation function calculations were done with computing resources provided by :



RIKEN BNL
Research Center

XSEDE
Extreme Science and Engineering
Discovery Environment

- M.L. is supported by SciDAC-3 and Argonne Leadership Computing Facility.